

 Open access • Journal Article • DOI:10.1002/ADMA.200306052

Preparation of arrays of isolated spherical cavities by self-assembly of polystyrene spheres on self-assembled pre-patterned macroporous films — [Source link](#)

Mamdouh E. Abdelsalam, Philip N. Bartlett, Jeremy J. Baumberg, S. Coyle

Institutions: University of Southampton

Published on: 05 Jan 2004 - Advanced Materials (WILEY-VCH Verlag)

Related papers:

- [Nanosphere lithography: A materials general fabrication process for periodic particle array surfaces](#)
- [Edge spreading lithography and its application to the fabrication of mesoscopic gold and silver rings.](#)
- [Nanosphere Lithography: A Versatile Nanofabrication Tool for Studies of Size-Dependent Nanoparticle Optics](#)
- [Optical properties of nanostructured metal films](#)
- [Electrochemical deposition of macroporous platinum,palladium and cobalt films using polystyrene latex sphere templates](#)

Share this paper:    

View more about this paper here: <https://typeset.io/papers/preparation-of-arrays-of-isolated-spherical-cavities-by-self-45qmsinrfz>

Experimental

For the fabrication of n-ZnO/p-GaN heteroepitaxial nanorod EL devices, n-ZnO nanorods were vertically grown on 3 μm thick p-GaN layers coated on Al₂O₃ (0001) using catalyst-free MOVPE. The p-GaN layers exhibited a p-type carrier concentration of $2 \times 10^{17} \text{ cm}^{-3}$ and a mobility of $10 \text{ cm}^2 \text{ V}^{-1} \text{ s}^{-1}$. For ZnO nanorod MOVPE growth, diethyl-zinc (DEZn) and oxygen were employed as reactant sources, as previously reported [13]. Details in the growth parameters of ZnO nanorods on GaN substrates are the same as those on sapphire substrates except for the DEZn flow prior to ZnO growth. That is, in the initial ZnO growth stage, only DEZn with a carrier gas flowed for 30 s prior to ZnO nanorod growth in order to prevent GaN surface oxidation.

The EL devices were fabricated by making good ohmic contacts on both p-GaN and n-ZnO. The ohmic contact on p-GaN was fabricated by evaporating Pt and Au bilayers. The typical Pt and Au layer thicknesses were 100 Å and 500 Å, respectively. After the metallization of p-GaN, the free space between the individual ZnO nanorods was filled with a thin photoresist by spin coating. This was followed by selective etching of the photoresist under an oxygen plasma in order to produce a nanorod array embedded in the photoresist with only the nanorod tips exposed (by 50–100 nm; Fig. 1c). For the metallization of the n-ZnO nanorods, 100 Å thick Ti and 500 Å thick Au layers were deposited on the nanorod tips through a shadow mask by electron-beam evaporation, resulting in a continuous contact layer on the ZnO nanorods (Fig. 1d). Good ohmic contacts on both n-ZnO and p-GaN were made by rapid thermal annealing at 300 and 500 °C for 1 min, respectively. The EL and *I*-*V* characteristics of the devices were measured by applying a DC voltage to the device using a source meter (Keithley 2400). The EL spectra were measured using a monochromator and a detection system equipped with a photomultiplier tube and a photon counter which had been used for photoluminescence spectroscopy [3]. All measurements were performed at room temperature.

Received: July 21, 2003

Final version: September 30, 2003

- [1] W. Y. Liang, A. D. Yoffe, *Phys. Rev. Lett.* **1968**, *20*, 59.
- [2] P. Zu, Z. K. Tang, G. K. L. Wong, M. Kawasaki, A. Ohtomo, H. Koinuma, Y. Segawa, *Solid State Commun.* **1997**, *103*, 459.
- [3] S. W. Jung, W. I. Park, H. D. Cheong, G.-C. Yi, H. M. Jang, S. Hong, T. Joo, *Appl. Phys. Lett.* **2002**, *80*, 1924.
- [4] M. H. Huang, S. Mao, H. Feick, H. Yan, Y. Wu, H. Kind, E. Weber, R. Russo, P. Yang, *Science* **2001**, *292*, 1897.
- [5] W. I. Park, Y. H. Jun, S. W. Jung, G.-C. Yi, *Appl. Phys. Lett.* **2003**, *82*, 964.
- [6] W. I. Park, G.-C. Yi, M. Kim, S. J. Pennycook, *Adv. Mater.* **2003**, *15*, 526.
- [7] R. D. Vispute, V. Talyansky, S. Choopun, R. P. Sharma, T. Venkatesan, M. He, X. Tang, J. B. Halpern, M. G. Spencer, Y. X. Li, L. G. Salamanca-Riba, A. A. Iliadis, K. A. Jones, *Appl. Phys. Lett.* **1998**, *73*, 348.
- [8] S.-K. Hong, T. Hanada, H. Makino, Y. Chen, H.-J. Ko, T. Yao, A. Tanaka, H. Sasaki, S. Sato, *Appl. Phys. Lett.* **2001**, *78*, 3349.
- [9] a) X. Duan, Y. Huang, Y. Cui, J. Wang, C. M. Lieber, *Nature* **2001**, *409*, 66. b) X. Duan, Y. Huang, R. Agarwal, C. M. Lieber, *Nature* **2003**, *421*, 241.
- [10] M. W. Wang, J. O. McCaldin, J. F. Swenberg, T. C. McGill, R. J. Hausnstein, *Appl. Phys. Lett.* **1995**, *66*, 1974.
- [11] G. D. J. Smit, S. Rogge, T. M. Klapwijk, *Appl. Phys. Lett.* **2002**, *81*, 3852.
- [12] W. I. Park, G.-C. Yi, J.-W. Kim, S.-M. Park, *Appl. Phys. Lett.* **2003**, *82*, 4358.
- [13] W. I. Park, D. H. Kim, S.-W. Jung, G.-C. Yi, *Appl. Phys. Lett.* **2002**, *80*, 4232.

- [14] D. C. Reynolds, D. C. Look, B. Jogai, *J. Appl. Phys.* **2001**, *89*, 6189.
- [15] M. A. Reshchikov, G.-C. Yi, B. W. Wessels, *Phys. Rev. B* **1999**, *59*, 13 176.
- [16] M. Kim, W. I. Park, G.-C. Yi, unpublished.
- [17] J. Neugebauer, C. G. Van de Walle, *Phys. Rev. Lett.* **1995**, *75*, 4452.
- [18] S. Sze, *Physics of Semiconductor Devices*, 2nd ed., Wiley, New York **1981**, Ch. 2.
- [19] T. Nakayama, M. Murayama, *J. Cryst. Growth* **2000**, *214*, 299.

Preparation of Arrays of Isolated Spherical Cavities by Self-Assembly of Polystyrene Spheres on Self-Assembled Pre-patterned Macroporous Films

By Mamdouh E. Abdelsalam, Philip N. Bartlett,*
Jeremy J. Baumberg, and Steve Coyle

Self-assembly of colloidal spheres onto patterned (e.g., lithographically modified)^[1] substrates is a promising approach to prepare complex three-dimensional (3D) geometries (e.g., assemble colloidal spheres into square pyramidal shapes)^[2] that cannot be produced by self-assembly of colloidal spheres on flat substrates. Generally self-assembly alone is restricted to the formation of close-packed two-dimensional (2D) and 3D arrays of colloidal particles and does not lead to more complex lattice types and geometries. A certain degree of control over colloidal self-assembly has been achieved through external electric^[3] or intense optical fields^[4] and by manipulating the interaction potential.^[5] Here, we demonstrate a simple scheme that combines two self-assembly steps and electrochemical deposition to produce patterns of ordered arrays of spheres with controlled spacing and eventually isolated metallic arrays of spherical cavities. First, the substrate was pre-patterned by electrochemical deposition through templates of polystyrene spheres assembled as a hexagonal-close-packed monolayer on an evaporated gold surface. This was followed by removal of the template by dissolution in tetrahydrofuran (THF). Then monodisperse polystyrene spheres were allowed to slowly assemble on the pre-patterned substrate in a purpose-built cell. Finally, electrochemical deposition through the top layer of spheres was achieved to produce the final 3D structure; the schematic illustration of this procedure is shown in Figure 1. Electrochemical deposition has a number of significant advantages. It produces a high density deposited material and no shrinkage of the material takes place when the template is removed.

[*] Prof. P. N. Bartlett, Dr. M. E. Abdelsalam
School of Chemistry, University of Southampton
Southampton, SO17 1BJ (UK)
E-mail: P.N.Bartlett@soton.ac.uk
Prof. J. J. Baumberg, S. Coyle
School of Physics and Astronomy
University of Southampton
Southampton, SO17 1BJ (UK)

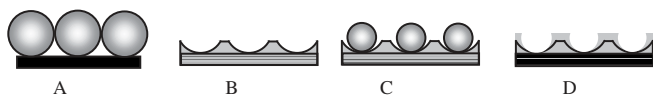


Figure 1. Schematic illustration of the procedure involved in the self-assembly of polystyrene spheres on a pre-patterned macroporous film. A) Assembly of polystyrene spheres on an evaporated gold surface. B) Electrochemical deposition through the polystyrene spheres template to pattern the substrate. C) Assembly of polystyrene spheres on patterned substrate. D) Electrochemical deposition through the top layer of spheres.

Also, it can be used to prepare a wide range of materials and allows fine control over the thickness of the resulting macroporous film through control of the total charge passed to deposit the film.^[6] The ability to build up such complex geometries plays an extremely important role in elucidating and understanding the optical and magnetic properties of these porous materials and their diverse applications.

Templating has been explored by a number of groups as a powerful means to pattern flat substrates and subsequently direct and control assembly processes. For example, Lieber and co-workers^[7] exploited assembly of nanowires (NWs) as masks for patterning lines with nanometer to micrometer scale pitches hierarchically over large areas. Self-assembly of colloidal particles produces close packed arrays that can be useful in themselves or can serve as templates for making more complex structures. Arrays of particles of this type, one or two layers thick, have been used as masks in lithographic processes where material was either deposited through the layer or the layer was used as an etch resist.^[8] Also infiltration of the spaces between the colloidal particles in the template by electrochemical deposition introduces a controllable way to pattern the substrates.^[9] In this part we first present our technique for self-assembly of colloidal layers. Strong capillary forces that develop at a meniscus between a substrate and a colloidal solution can be used to produce 3D arrays of controlled thickness.^[10–15] If this meniscus is slowly swept across a vertically placed substrate by, for example, solvent evaporation, thin planar opaline films can be deposited. A modification of this approach was used in the present work using cysteamine-modified gold surfaces. The formation of close-packed monolayers or multilayers of colloidal particles on the modified gold surface was achieved by changing the concentration of the polystyrene suspension or by repeating the assembly process several times. In a first self-assembly step the deposition of the colloidal template layers was carried out in a thin layer cell (2 cm × 1.5 cm) made up of a cysteamine-coated gold electrode and a clean uncoated glass plate, held 100 μm apart by a spacer cut from Parafilm. The space between the two plates was filled with the aqueous suspension of polystyrene latex spheres. The transparent glass plate allows the filling of the cell to be monitored and a very slight argon stream was used to remove any trapped air bubbles. The filled thin layer cell was held vertically in an incubator in order to control the rate of evaporation from the cell. After drying the template appears opalescent with colors from

green to red, depending on the angle of observation, clearly visible when illuminated from above with white light. The arrangement of the spheres in the template films was investigated using high-magnification scanning electron microscopy (SEM). Figure 2A shows a top-view of a typical template assembled from 700 nm polystyrene spheres on a cysteamine-treated gold surface. The spheres are close-packed in a well

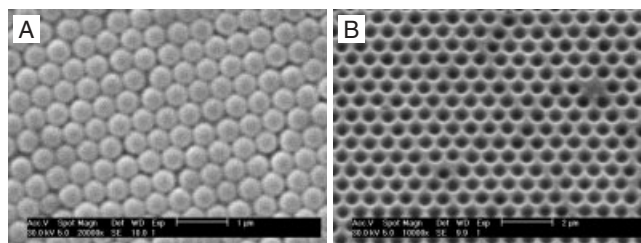


Figure 2. SEM images of the template and the templated gold films. A) Template assembled from 700 nm diameter polystyrene spheres. B) A 170 nm thick gold film electrodeposited through a 700 nm sphere diameter template.

ordered hexagonal array. These templates are robust and adhere well to the gold substrates. Gold films of controlled thickness were electrochemically deposited, at a potential of -1 V versus SCE (SCE: saturated calomel electrode), from an aqueous gold plating solution through the pre-assembled template. Figure 2B shows a typical SEM image of a templated gold film 170 nm thick grown through a template made up of a monolayer of 700 nm diameter polystyrene spheres. The micrograph shows that the spherical segment voids left in the gold film after the removal of the polystyrene spheres have smooth and uniform mouths and are arranged in a well ordered, close-packed array as expected from the structure of the original template. The center-to-center distance measured for the pores in the film shown in Figure 1B, and for similar SEM images of other films, is the same as the diameter of the polystyrene spheres used to prepare the template; thus the diameter of the spherical segment voids within the gold film is directly determined by the diameter of the polystyrene spheres used to form the template. Consequently, the periodic dimension of the templated film can be changed by using polystyrene spheres of different size to control the center-to-center distance. In addition, the film thickness and the pore mouth diameter can be adjusted through control of the total charge passed to deposit the film.

In a second self-assembly step, monodisperse polystyrene spheres were then allowed to slowly assemble on the pre-patterned substrate in a cell similar to that used in the first assembly step. The patterned substrate was again coated with cysteamine and clamped to a clean uncoated glass plate with a Parafilm spacer. The space between the two substrates was filled with the aqueous suspension of polystyrene latex spheres. The filled cell was held tilted at 60° , with the patterned substrate on the lower side, in an incubator in order to control the rate of evaporation from the cell. As the liquid confined in the cell slowly evaporates the meniscus moves

across the patterned substrate and assembles the spheres so that they fill the pores in the substrate. The efficiency of the assembly process is determined by the gravitational force, the substrate–particle electrostatic interaction, and the capillary forces.^[2] The gravitational force is less significant for polystyrene spheres because their density ($\sim 1.05 \text{ g cm}^{-3}$) is close to that of water ($\sim 1.00 \text{ g cm}^{-3}$). In this case, the electrostatic interaction between the particles and the substrate is attractive. This is because the substrate surface is positively charged as a result of the chemical modification with the cysteamine, and the spheres have a negative surface charge due to the sulfate groups used to stabilize the polystyrene suspension.^[16] Finally, the capillary immersion force arises when the tops of spheres protrude from the thin liquid film formed at the interface between liquid and substrate. These forces depend on the wetting properties of the substrates, i.e., the magnitude of the contact angle and the distance between the spheres.^[17–20] The meniscus formed between the spheres and the substrate and that formed between the spheres produce substantial forces that direct the spheres to fill the pores of the patterned substrate. Optimizing the parameters involved in the second assembly steps, e.g., the concentration of the colloidal particles and the evaporation rate, we have been able to almost completely fill the pores ($> 90\%$) of the patterned substrate. The domain sizes measured over the whole area of the patterned substrate ranged from 100 to 5000 μm .

The structured arrangement of the assembled spheres on top of the patterned substrate is controlled by the ratios between the center-to-center distances for the pores and the size of the assembled spheres. Simply by varying these ratios it is possible to obtain different structures. Figure 3A shows an SEM image of 700 nm diameter polystyrene spheres assembled on a gold macroporous patterned film prepared by electrodeposition through a template made of 700 nm polystyrene spheres. It can be seen that the spheres are assembled as a hexagonal-close-packed layer on top of the pores of the patterned substrate. The spheres in the top layer are in physical contact with each other, as shown in the insert of the Figure 3A, because the center-to-center periodicity of the film exactly matches the sphere diameter. Figures 3B,C show the assembly of 900 nm and 500 nm diameter polystyrene spheres on a gold macroporous patterned film prepared by electrodeposition through a template made of 700 nm polystyrene spheres. In Figure 3B, the spheres are bigger than the center-to-center periodicity of the substrate therefore the spheres in the top layer are not well ordered, aggregating in local clusters. In contrast, when the sphere diameter is smaller than the center-to-center periodicity of the substrate (Fig. 3C) the spheres assemble in a well ordered array but the spheres are not close packed, i.e., they do not touch each other. This offers a simple way to produce ordered arrays of spheres with controlled spacing.

Electrodeposition around the spheres assembled on the patterned substrates produces a structured film. Figure 3D shows the resulted electrochemical deposition of gold through the template shown in Figure 3C. Metallic arrays of isolated spherical cavities were produced. The pore mouth diameter was 480 nm and center-to-center distance was 701 nm.

In conclusion, the combination of self-assembly and electrochemical deposition provide a simple scheme that can be used to pattern flat substrates. Then, in a second self-assembly step polystyrene spheres were allowed to assemble on the pre-patterned substrate. The structural arrangement of the assembled spheres can be changed by changing the ratio between the center-to-center distances for the pores and the size of the spheres. Electrodeposition around the spheres assembled on the patterned substrates produces a structured film. Following these steps we succeeded to produce isolated metallic arrays of spherical cavities. The ability to easily fabricate, at low cost, a large variety of such photonic metallic structures promises applicability in many diverse areas, ranging from biotechnology to optoelectronics.

Experimental

The templates were made from monodisperse polystyrene latex spheres (Duke Scientific Corporation) supplied as a 1 wt.-% solution in water (manufacturer's certified mean diameter of $701 \pm 6 \text{ nm}$, $895 \pm 8 \text{ nm}$, and $499 \pm 5 \text{ nm}$ and coefficient of variation in diameter 1.3% in all cases). Before use, the suspensions were homogenized by successive, gentle inversions for a couple of minutes followed by a sonication for 30 s.

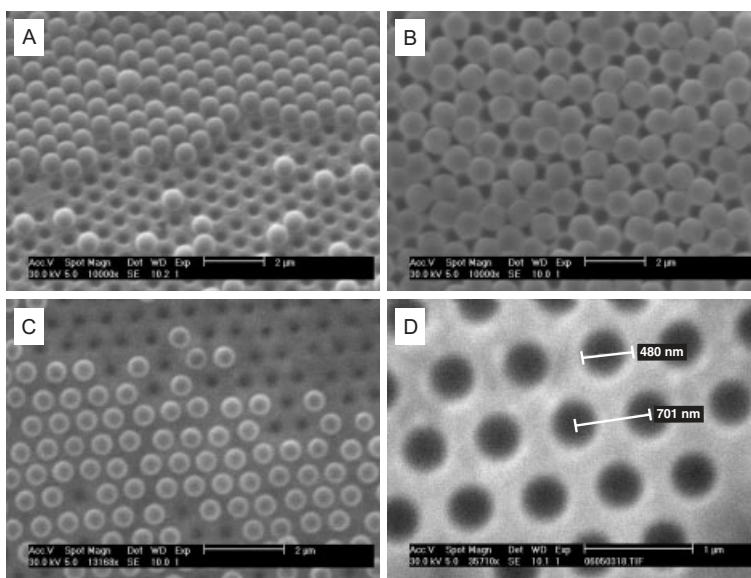


Figure 3. Assembly of polystyrene spheres on a gold macroporous patterned film prepared by electrodeposition through a template made of 700 nm polystyrene spheres. A) Polystyrene spheres of 700 nm diameter assembled on a substrate of 500 nm pore diameter; the inset, a top view, shows how the spheres touch each other. B) Polystyrene spheres of 900 nm diameter assembled on a substrate of 690 nm pore diameter. C) Polystyrene spheres of 500 nm diameter assembled on a substrate of 400 nm pore diameter and 70 nm thick. D) Gold film prepared by electrodeposition through the template shown in (C), pore diameter of the top film is 480 nm and center-to-center distance is 701 nm.

All solvents and chemicals were of reagent quality and were used without further purification. The commercial cyanide free gold plating solution (Tech. Gold 25, containing 7.07 g dm^{-3} gold) was obtained from Technic Inc. (Cranston, R.I.). Isopropanol, cysteamine, and ethanol were obtained from Aldrich. THF was obtained from Fisher Chemicals. All solutions were freshly prepared using reagent-grade water ($18 \text{ M}\Omega \text{ cm}$) from a Whatman RO80 system coupled to a Whatman "Still Plus" system.

Evaporated gold electrodes, used as substrates, were prepared by evaporating 10 nm of chromium, followed by 200 nm of gold onto 1 mm thick glass microscope slides. These gold substrates were thoroughly cleaned before use by sonication in deionized water for 30 min, followed by sonication in isopropanol for 90 min. They were then rinsed with deionized water and dried under a gentle stream of argon (BOC Gases). Cysteamine was self-assembled onto the evaporated gold electrodes by immersing the freshly cleaned gold substrate in a 10 mmol dm^{-3} ethanolic solution of cysteamine at room temperature for several days.

Electrochemical deposition was performed in a thermostated cell at 25°C using a conventional three-electrode configuration controlled by an Autolab PGSTAT30. The template-coated gold substrate was the working electrode with a large area platinum gauze counter electrode and a home-made SCE. Gold films were deposited under potentiostatic conditions at -0.95 V versus SCE.

An environmental scanning electron microscope (Philips XL30 ESEM) was used to study the morphology and microstructure of both the polystyrene templates and the macroporous metal films.

Received: August 21, 2003

Final version: September 24, 2003

SiC–SiO₂–C Coaxial Nanocables and Chains of Carbon Nanotube–SiC Heterojunctions

By Yubao Li,* Yoshio Bando, and Dmitri Golberg

During the fast development of nanotechnology in the past decade, most of the research efforts have been focused on the preparation of nanometer-sized functional electronic devices. Joining multiple phases within a given one-dimensional nanostructure in its radial or axial direction results in the formation of two distinctive heterostructures, namely, coaxial nanocables or heterojunctions. Zhang et al. first reported a laser ablation process for the synthesis of SiC–SiO₂–BN/C nanocables and amorphous B–SiO₂–C nanocables.^[1,2] Shi et al.^[3] prepared a three-layer nanocable possessing a crystalline Si core, an amorphous SiO₂ intermediate layer, and an amorphous C outer sheath using a combined laser ablation and thermal evaporation technique. A standard route to prepare nanoscale heterojunctions is to produce the desired vapors and organize their flow during the nanostructure growth. Hu et al.^[4] reported the synthesis of the heterojunctions made of multi-walled carbon nanotubes (CNTs) and Si nanowires and on a reproducible rectifying behavior of this metal–semiconductor junction. Lu and workers^[5] synthesized Pt₆Si₅–Si heterojunctions using polycrystalline Pt nanowires as templates. GaAs–GaP nanowire heterojunctions were also prepared via a laser-assisted catalytic growth.^[6] Park et al.^[7] reported the synthesis of ZnO–ZnMgO heterojunctions displaying a quantum confinement effect. ZnO–Ni heterojunctions were prepared by depositing Ni at the tips of ZnO nanorods; these exhibited a metal-layer-thickness-dependent magnetic property.^[8] Another efficient route is based on solid-state reactions, as reported by Zhang et al., during the preparation of heterojunctions of single-walled CNTs and SiC/TiC through high-temperature reactions between CNTs and Si/Ti.^[9] CNTs have been shown to be versatile for many applications. The ballistic electron transport and excellent mechanical properties suggest that CNT-based nanostructures are most valuable for building novel electronic nanodevices. In this communication, we report a simple thermal evaporation route for the mass-production of SiC–SiO₂–CNT coaxial nanocables. Most importantly, we found that these nanocables may be further transformed into nanochains of SiC–CNT junctions during high-temperature annealing in vacuum.

As shown in Figure 1, only two phases, namely cubic β -SiC and CNTs, are detected in the X-ray diffraction (XRD) patterns of the as-synthesized and annealed samples. It is worth noting that the peaks characteristic of the SiC phase become

- [1] A. van Blaaderen, R. Ruel, P. Wiltzius, *Nature* **1997**, 385, 321.
- [2] Y. Yin, Y. Lu, B. Gates, Y. Xia, *J. Am. Chem. Soc.* **2001**, 123, 8718.
- [3] a) M. Trau, D. A. Saville, I. A. Aksay, *Science* **1996**, 272, 706.
b) S. R. Yeh, M. Seul, B. I. Shraiman, *Nature* **1997**, 386, 57.
- [4] M. M. Burns, J. M. Fournier, J. A. Golovchenko, *Science* **1990**, 249, 749.
- [5] a) C. A. Murray, D. H. van Winkle, *Phys. Rev. Lett.* **1987**, 58, 1200.
b) A. E. Larsen, D. G. Grier, *Nature* **1997**, 385, 230.
- [6] P. N. Bartlett, J. J. Baumberg, P. R. Birkin, M. A. Ghanem, M. C. Netti, *Chem. Mater.* **2002**, 14, 2199.
- [7] D. Whang, S. Jin, C. M. Lieber, *Nano Lett.* **2003**, 3, 951.
- [8] a) H. W. Deckman, J. H. Dunsmuir, *Appl. Phys. Lett.* **1982**, 41, 377.
b) F. Burmeister, C. Schäfle, B. Keilhofer, C. Bechinger, J. Boneberg, P. Leiderer, *Adv. Mater.* **1998**, 10, 495.
- [9] P. N. Bartlett, J. J. Baumberg, S. Coyle, M. E. Abdelsalem, *Faraday Discuss.* **2004**, 125, 117.
- [10] P. Jiang, J. F. Bertone, K. S. Hwang, V. L. Colvin, *Chem. Mater.* **1999**, 11, 2132.
- [11] A. S. Dimitrov, T. Miwa, K. Nagayama, *Langmuir* **1999**, 15, 5257.
- [12] A. S. Dimitrov, K. Nagayama, *Chem. Phys. Lett.* **1995**, 243, 462.
- [13] K. Nagayama, *Colloids Surf., A* **1996**, 109, 363.
- [14] A. S. Dimitrov, K. Nagayama, *Langmuir* **1996**, 12, 1303.
- [15] N. D. Denkov, O. D. Velev, P. A. Kralchevsky, I. B. Ivanov, H. Yoshimura, K. Nagayama, *Nature* **1993**, 361, 26.
- [16] *Science and Technology of Polymer Colloids* (Eds: G. W. Poehlein, R. H. Ottewill, J. W. Goodwin), Vol. II, Martinus Nijhoff, Boston, MA **1983**.
- [17] P. A. Kralchevsky, K. Nagayama, *Langmuir* **1994**, 10, 23.
- [18] P. A. Kralchevsky, V. N. Paunov, I. B. Ivanov, K. J. Nagayama, *J. Colloid Interface Sci.* **1992**, 151, 79.
- [19] P. A. Kralchevsky, V. N. Paunov, N. D. Denkov, I. B. Ivanov, K. J. Nagayama, *J. Colloid Interface Sci.* **1993**, 155, 420.
- [20] N. D. Denkov, O. D. Velev, P. A. Kralchevsky, I. B. Ivanov, H. Yoshimura, K. Nagayama, *Langmuir* **1992**, 8, 3183.

[*] Dr. Y. B. Li, Prof. Y. Bando, Dr. D. Golberg
National Institute for Materials Science
Advanced Materials Laboratory
Namiki 1–1, Tsukuba, Ibaraki 305–0044 (Japan)
E-mail: Li.Yubao@nims.go.jp